PHAST VALIDATION OF DISCHARGE AND ATMOSPHERIC DISPERSION FOR PRESSURISED CARBON DIOXIDE RELEASES

Henk W.M. Witlox, Mike Harper and Adeyemi Oke
DNV Software, London, UK

The consequence modelling package Phast examines the progress of a potential incident from the initial release to the far-field dispersion including the modelling of rainout and subsequent vaporisation. The original Phast discharge and dispersion models allow the released chemical to occur only in the vapour and liquid phases. The latest versions of Phast include extended models which also allow for the occurrence of fluid to solid transition for carbon dioxide (CO_2) releases.

As part of BP's engineering project DF1 (made publicly available via CO2PIPETRANS JIP), experimental work on CO_2 releases was carried out at the Spadeadam site (UK) by Advantica for BP. These experiments included both high-pressure steady-state cold releases (liquid storage) and high-pressure time-varying supercritical hot releases (vapour storage). The CO_2 was stored in a vessel with attached pipework. At the end of the pipework a nozzle was attached, where the nozzle diameter was varied.

This paper discusses the validation of Phast against the above experiments. The flow rate was very accurately predicted by the Phast discharge models within the accuracy at which the experimental data were measured. The concentrations were found to be predicted accurately (well within a factor of two) by the Phast dispersion model (UDM). This validation was carried out with no fitting whatsoever of the Phast extended discharge and dispersion models.

1. INTRODUCTION

This paper discusses the validation of discharge and subsequent atmospheric dispersion for pressurised carbon dioxide releases using the consequence modelling package Phast based on experimental data shared by the CO2PIPETRANS JIP.

Phast examines the progress of a potential incident from the initial release to the far-field dispersion including the modelling of rainout and subsequent vaporisation. The original Phast discharge and dispersion models allow the released chemical to occur only in the vapour and liquid phases. The models in the latest versions 6.6 and 6.7 of Phast were extended by Witlox *et al*. (2009) to also allow for the occurrence of fluid to solid transition for CO_2 releases. This applies both for the post-expansion state in the discharge model, as well as for the thermodynamic calculations by the dispersion model. The extended dispersion formulation was tested extensively by means of a sensitivity analysis for a comprehensive range of base cases (Witlox *et al*., 2010).

The Phast dispersion model (UDM) was previously validated for unpressurised releases of CO_2, i.e. against the McQuaid wind-tunnel experiments for isothermal heavy-gas-dispersion from a ground-level CO_2 line source (Witlox and Holt, 1999), the Kit Fox experiments for heavy-gas-dispersion from a ground-level areas source (Witlox and Holt, 2001), and the CHRC wind-tunnel experiments for a CO_2 ground-level vapour pool source (Witlox, Harper and Pitblado, 2012). The focus of the current paper is validation of Phast against pressurised CO_2 experiments.

As part of BP's engineering project DF1, experimental work on CO_2 releases was carried out at the Spadeadam site (UK) by Advantica (now part of GL Noble Denton) for BP. These experiments included both high-pressure steady-state cold releases (liquid storage) and high-pressure supercritical time-varying releases (vapour storage). The CO_2 was stored in a vessel with attached pipework. At the end of the pipework a nozzle was attached, where the nozzle diameter was varied. For the cold releases the pressure was kept constant. The results of this experimental work are reported in the Advantica report by Evans and Graham (2007) and the DF1 close-out report by Holt (2012). BP, when joining the DNV led CO2PIPETRANS Phase 2 Joint Industry Project (JIP), transferred the DF1 CO_2 experimental work to the JIP. As part of this JIP's goal to reduce uncertainty associated with CO2 pipeline design and operation the majority of the DF1 data was made available in the public domain.

The current paper discusses the validation of Phast against the above BP experiments. In Section 2 first a brief overview is provided for Phast modelling of discharge and dispersion for CO_2 releases. Section 3 subsequently describes the BP DF1 experiments. Section 4 describes the validation of the Phast steady-state discharge model DISC and the Phast time-varying discharge model TVDI against the BP experiments. Section 5 outlines the validation of Phast dispersion model UDM adopting the source-term data derived from DISC and TVDI.

The reader is referred to the detailed data review report by Witlox (2012) for further detailed results not included in the current paper.

2. OVERVIEW OF PHAST MODELLING OF DISCHARGE AND DISPERSION FOR CO_2 RELEASES

Figure 1 includes a schematic phase diagram for CO_2; CO_2 has a critical temperature of 31.06C (304.2K) above which

it is always vapour and a triple point of 5.1 atmosphere and − 56.55C (216.6K) below which all non-vapour CO_2 will be solid.

Phast examines the progress of a CO_2 release from the initial release to far-field dispersion including the modelling of solid rainout and subsequent sublimation to vapour. The main areas for modelling of CO_2 in Phast as shown in Figure 2 are as follows:

- Discharge modelling of CO_2 which includes atmospheric expansion of CO_2 (depressurisation to ambient pressure) during which liquid to solid/vapour expansion occurs. In case of initial supercritical temperature (above 31°C), vapour to vapour, or vapour to solid/vapour expansion occurs.

  The applied Phast discharge models are DISC (steady-state cold releases) and TVDI (time-varying hot releases). Starting from the specified vessel stagnation conditions, the discharge model DISC/TVDI is used for modelling the discharge of the CO_2. This includes expansion from storage conditions to orifice conditions, and the expansion from orifice to ambient conditions. For the latter expansion the DISC/TVDI sub-model ATEX is used.
- Dispersion modelling involving the possible presence of solid CO_2 in addition to vapour CO_2.

  The ATEX post-expansion conditions are used as the source term (starting condition) for the UDM dispersion model. The UDM calculates the CO_2 dispersion further downwind ignoring possible deposition on the ground and re-sublimation. The UDM assumes that the release direction is in the same vertical plane as the wind direction.

The UDM model invokes a thermodynamics sub-model for mixing of the released material and the ambient air. This model calculates the phase composition and temperature of the mixture at the cloud centre-line. For the BP DF1 CO_2 experiments the stagnation pressures are very large and therefore the initial solid particle is expected to be very small (initial fine mist of CO_2). Furthermore the atmospheric boiling point is very low (−78.4°C) and therefore the solid particles are expected to sublime very fast. As a result for the mixing of solid/vapour CO_2 with air, the UDM thermodynamics sub-model assumes homogeneous equilibrium without deposition of the solid CO_2 onto the substrate. Thus trajectories of solid particles are not modelled. The latter assumption was further verified by a detailed sensitivity analysis by Witlox *et al*. (2010).

The reader is referred to Witlox *et al*. (2009) for further details of the modelling.

3. BP EXPERIMENTS

Experiments involving pressurised CO_2 releases were carried out at Spadeadam by Advantica for BP in 2006. The data from these experiments along with other material was transferred into the DNV led CO2PIPETRANS JIP. DNV Software was commissioned by the JIP to undertake a critical review of the tests that were considered suitable for model validation, i.e. those corresponding to horizontal non-impinging releases, before the data from these tests were approved for external release. The data review (Witlox, 2012) was carried out based on the information provided by the CO2PIPETRANS JIP [Advantica report by Evans and Graham (2007) and the DF1 overview

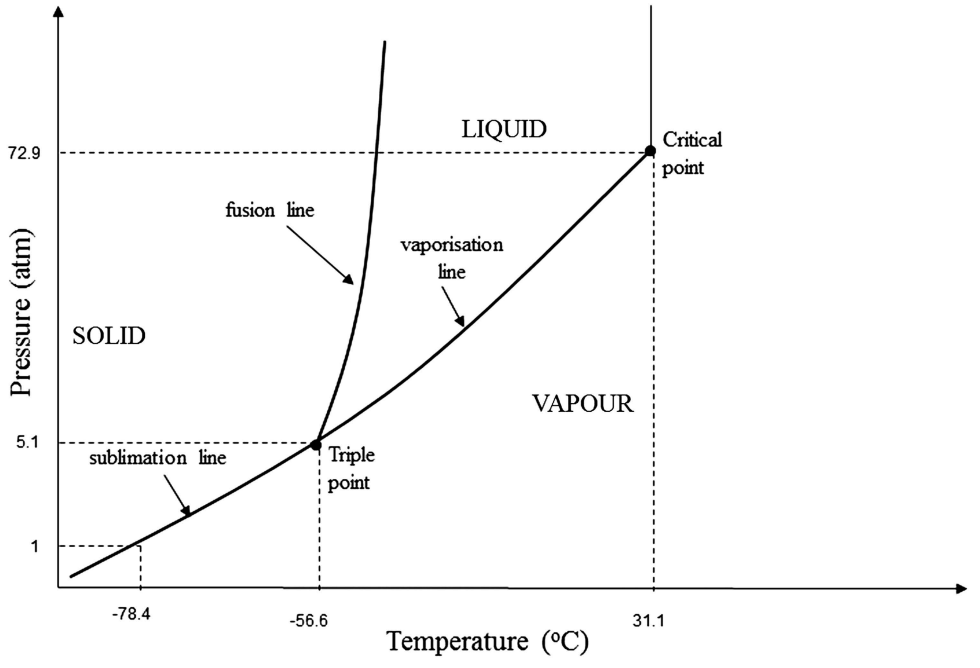

Figure 1. Schematic phase diagram for CO_2 (not on scale)

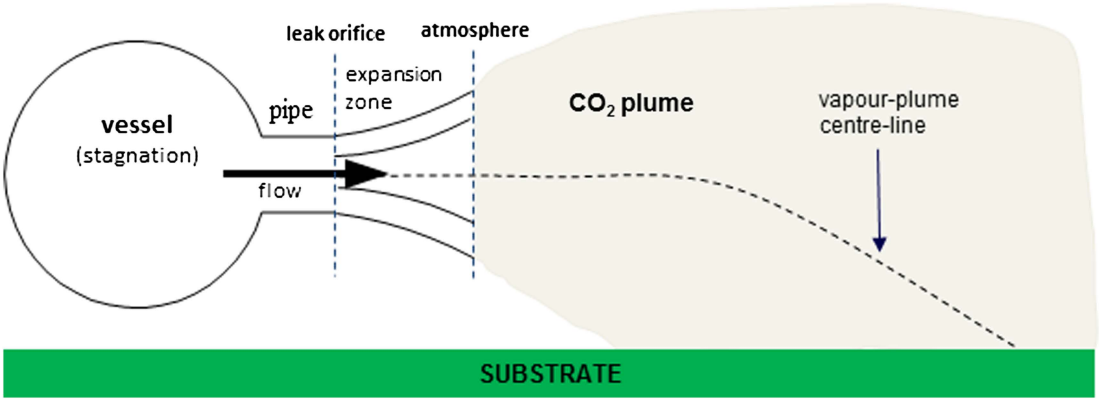

Figure 2. Discharge modelling (DISC/TVDI/ATEX) and dispersion modelling (UDM)

report by Holt (2012)] as well as some supplementary information provided by the original 2006/2007 BP model validation exercise.

In the experiments the CO_2 was stored in a horizontal cylindrical vessel. The modelled experiments include two sets of experiments:

- High-pressure cold steady-state releases (liquid storage; tests 1, 2, 3, 5, 6, 11). For these tests nitrogen padding gas was used to maintain the pressure in the vessel and to keep the test vessel full of liquid CO_2.
- High-pressure hot supercritical time-varying releases (dense vapour storage; tests 8, 8R, 9). For these tests the vessel was first filled with CO_2 at the required test pressure and test temperature. The CO_2 was heated using heating pads. Subsequently the CO_2 was released through the nozzle driven only by the pressure in the vessel with the vessel pressure decaying as the release progressed.

Downstream of the vessel a 3 m horizontal flexible hose was attached (2″ inner diameter), connected to a 2 m 2″ metering spool and a 0.5 m 2″ nozzle with an orifice plates bolted on the nozzle. Thus the total length of attached pipe is 5.5 meter, with no external insulation applied to the pipe. A range of orifice diameters was applied i.e. 25.62 mm, 11.94 mm and 6.46 mm with orifice lengths of 72.41 mm, 46.78 mm and 47.79 mm, respectively.

Table 1 summarises the key experimental data required as input to the Phast models. In this table the values of the storage pressure and the storage temperature are taken at the discharge end of the vessel (upstream of the pipework), with mean values during the release applied for the steady-state liquid releases and with initial values applied for the transient vapour releases. The ambient data were measured upwind of the release and mean values are adopted for these data during the release. This is with the exception of the wind-speed measurement of 1.65 m above the pad, which was taken 40 m downwind of the release. Since this measurement was disturbed by the CO_2 jet, the value listed in Table 1 corresponds to the mean value prior to the release. Furthermore, based on an analysis of the experimentally observed vertical wind-speed profiles a surface roughness of 0.1 m and a stability class of D was assumed for all tests. Finally with respect to the wind direction it is noted that the release direction corresponds to 270°.

4. VALIDATION OF PHAST DISCHARGE MODELS AGAINST BP EXPERIMENTS

For the supercritical vapour releases, the flow rate was derived from the measured vessel weight using load cells. For the cold liquid releases, the flow rate was estimated by Advantica (Evans and Graham, 2007) from the load cells by assuming that the total vessel mass M (as measured by the load cells, kg) equals $M = \rho_{CO2}V_{CO2} - \rho_{N2}V_{N2}$. Here ρ_{CO2} is the CO_2 density (kg/m^3), V_{CO2} the CO_2 volume rate (kg/s), ρ_{N2} the nitrogen density (kg/m^3), and V_{N2} the nitrogen volume flow rate (kg/s). Pressure and temperatures were measured at a range of locations upstream of the vessel, inside the vessel, and downstream of the vessel along the pipe and the release valve.

The Phast discharge models either assume the release to be directly from an orifice from a vessel (‘Leak’ scenario), or from a short pipe attached to a vessel (with orifice diameter = pipe diameter, i.e. full-bore rupture). Except for test 5 (1″ orifice), the observed pressure at the discharge end was seen to be very close to the observed pressure at the vessel inlet and vessel outlet. Thus the Phast ‘Leak’ scenario was applied, while neglecting the pressure loss from the stagnation conditions to the nozzle conditions. The Phast discharge model DISC was used to simulate the steady-state liquid releases, while the Phast discharge model TVDI was used to model the time-varying vapour releases. Default Phast parameters were applied with two exceptions. First the metastable assumption (non-equilibrium with liquid ‘frozen’) was not applied for the DISC simulations, but flashing was allowed at the orifice (equilibrium at the orifice) to account for the pipework upstream of the orifice. Secondly conservation of

Table 1. Experimental conditions for CO_2 tests

Input	Test1	Test2	Test3	Test5	Test6	Test11	Test8	Test8R	Test9	Input for models
Discharge data										
steady-state/transient	steady	steady	steady	steady	steady	steady	trans.	trans.	trans.	–
storage phase	liquid	liquid	liquid	liquid	liquid	liquid	vapour	vapour	vapour	DISC, TVDI
storage pressure (barg)	103.4	155.5	133.5	157.68	156.7	82.03	157.76	148.7	154.16	DISC, TVDI
storage temperature (C)	5	7.84	11.02	9.12	9.48	17.44	147.12	149.37	69.17	DISC, TVDI
vessel volume (m^3)	–	–	–	–	–	–	6.3	6.3	6.3	TVDI
orifice diameter (mm)	11.94	11.94	11.94	25.62	6.46	11.94	11.94	11.94	11.94	DISC, TVDI
release duration (s)	60	59	60	40	120	58	120	132	179	–
Ambient data										
ambient temperature (C)	14.2	7.5	10.6	5.8	6.1	11.6	11.19	11.1	8.2	DISC, TVDI, UDM
ambient pressure (mbara)	999.4	958.2	972.5	985.4	938.4	960.2	957.99	957.1	958.9	DISC, TVDI, UDM
relative humidity (%)	74.4	96	95.8	96.7	1	94	100	100	99.9	DISC, TVDI, UDM
wind direction (degrees)	322.4	265.6	288.8	278.6	299	270.8	269.3	270	270.7	UDM uses 270°
wind speed (m/s)	4	3.44	3.37	5.13	2.20	5.99	4.71	0.76	4.04	UDM

momentum was applied for the expansion from orifice to post-expansion conditions, since this assumption was previously found to provide the most accurate concentration predictions [e.g. against the SMEDIS experiments; see the UDM validation manual (Witlox, Harper and Holt, 2011) for details].

Figure 3 illustrates very close agreement between TVDI-predicted and observed values for expelled mass (kg) and flow rate (kg/s) for the time-varying tests 8, 8R and 9. In these curves, the solid lines refer to the experimental results and the dashed lines to the TVDI predictions. The experimentally observed values for the flow rates are averaged over a period over 8 seconds to reduce oscillations caused by inaccuracies of the load-cell measurements.

Table 2 summarises the overall results of the discharge rates for all tests. For the steady-state tests only the DISC initial release rate is given, while for the time-varying releases also the TVDI-predicted averaged release rate over the first 20 seconds is indicated. It is noted that the difference between the averaged rate and the initial rate is relatively small. From the table it is seen that the time-varying Phast predictions align well with the observed discharge rate for the hot tests 8, 8R and 9. The predicted flow rate for the cold releases, with the exception of test 5 (1″ release), is also very close to that of the experiments.

For test 5 (1″ release) the flow rate is over-predicted with 23% (50.74 kg/s predicted versus 41.17 kg/s experimental) using the 'Leak' scenario, while using the pipe ('Line Rupture') scenario it is under-predicted with 34.5% (26.95 kg/s predicted versus 41.17 kg/s). The over-prediction for the orifice scenario is believed to be caused by the fact that pressure loss is ignored along the pipework (hose/spool/nozzle). Test 5 has the largest orifice diameter (1″) and therefore will be most susceptible to upstream pressure loss and reduced flow rate. Indeed if a more accurate pressure would be applied of 128.6 barg (corresponding to averaged observed pressure close to the orifice) a release rate of 45.34 kg/s is predicted using the 'Leak' scenario corresponding to a much smaller over-prediction of 10.1%.

The DISC input data for Test 6 are virtually identical to those for Test 2, with the exception of the orifice size. From the DISC results it is concluded, that the predicted flow rate Q (kg/s) is virtually exactly linear to the orifice area $A_{orifice}$, i.e.

$$Q_{test2}A_{orifice,\ test6}/A_{orifice,\ test2} = 3.214\ \text{kg/s} \approx Q_{test6} = 3.212\ \text{kg/s}.$$

EVALUATION OF SOURCE TERMS FOR UDM DISPERSION

As indicated above the flow rate changes little for the time-varying tests 8, 8R, 9 within the first 20 seconds, and it is believed that within 20 seconds the maximum concentrations will be achieved within the first 80 meter (given relatively large initial jet momentum and relatively large values of wind speed). Therefore in the next section the dispersion calculations are modelled as steady-state using the averaged flow rate over the first 20 seconds for tests 8, 8R and 9, while for the other tests the overall averaged observed value is adopted. All other UDM input data (temperature, solid fraction, velocity, droplet diameter) are chosen as predicted above by the discharge model DISC. The predicted 'droplet' (solid particle) diameter is in fact not actual input to the UDM calculations, since no particle deposition is assumed in the case of CO_2. However as indicated previously it would not affect the UDM predictions, since the solid very rapidly sublimes and no 'rainout' (solid deposition) occurs.

5. VALIDATION OF PHAST DISPERSION MODEL AGAINST BP EXPERIMENTS

The CO_2 concentration was largely measured via O_2 cells with two additional Servomex CO_2 analysers; see Figure 4 (taken from Evans and Graham, 2007) for the location of the concentration sensors. Thus a total of 43 sensors was applied at downstream distances of 5 m (sensor OC01), 10 m (OC02), 15 m (OC03), 20 m (OC04-OC08), 40 m (OC9-OC21), 60 m (OC22-OC28) and 80 m (OC29-OC43), with sensors position at a range of different heights (0.3, 1 or 3 m) and cross-stream distances (between −20 and +20 degrees from the release direction).

Phast assumes that the release direction is the same as the wind direction, while for some of the experiments (see Table 1) there is a significant deviation from the wind direction. This may lead to less accuracy of the predictions in the far-field but will not significantly affect the prediction for the momentum-driven dispersion in the near-field.

For the steady-state test 11 the averaged wind direction (270.8 degrees) is very close to the release direction (270 degrees). Figure 5 includes observed raw concentrations for sensors OC01, OC03 and OC16 locations at 5, 15 and 40 m downstream distances along the release axis and at 1 meter height. In addition it includes observed concentrations time-averaged over 11 seconds, 21 seconds and 59 seconds. Here 59 seconds approximately corresponds to the release duration (reported as 60 seconds).

Figure 5a shows that the concentration fluctuations are relatively small with respect to the mean concentration, and therefore a relatively accurate measurement of the concentration can be provided. This is also because the jet centre-line will pass sensor OC1 very closely. In theory (so close to the release point) the concentrations should be approximately constant over a period of 60 seconds (roughly between 75 seconds and 135 seconds). There is a relative small spread between the maximum value for 11-second averaged concentration (21.15 mol %) and the 59-second averaged concentration (18.79%).

The subsequent figures Figures 5b and 5c however show that the relative differences increase with increasing distance from the source. This is partly because the plume centre-line is more likely to miss the sensors at distances further downstream (because of fluctuating wind direction, as confirmed by wind direction variation observed by Advantica), and also because the sensor readings become

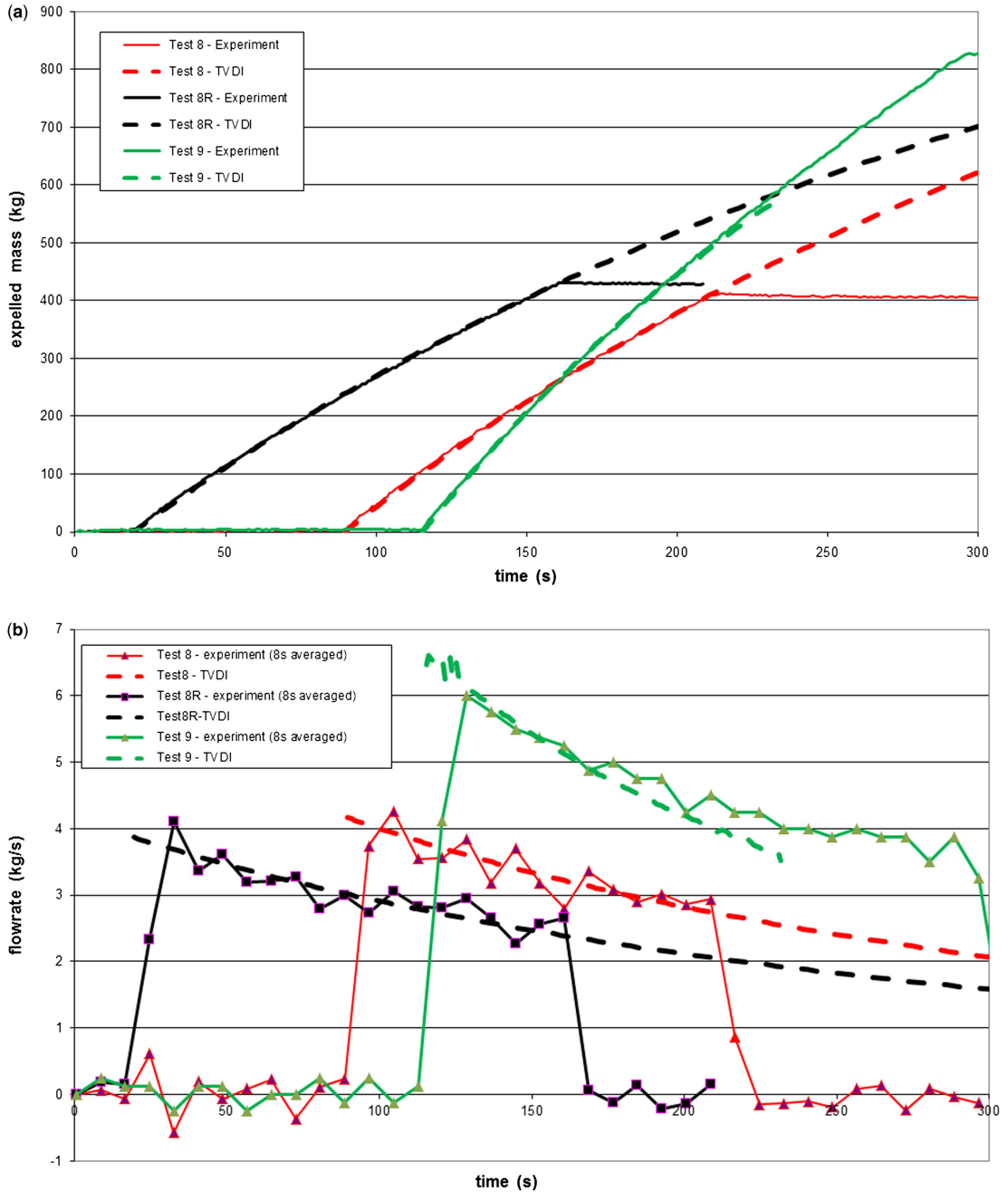

Figure 3. TVDI validation of expelled mass and flow rate (tests 8, 8R, 9) (a) expelled CO_2 mass, (b) CO_2 flow rate

relatively less accurate further downstream. For small concentrations, the sensor seems to have an accuracy of no better than 0.5%. Thus measurements with average concentrations less than 1% are considered to be of less value (except to confirm that the concentrations are small). Figure 5c shows that the concentration away from the plume is erroneously 'negative', and one may therefore consider to re-calibrate the observed concentrations (i.e. increase all measured values with the negative minimum value). However this has not been carried out as part of the current work.

Figure 6 plots for test 11 the maximum values over time of the measured concentration along with the Phast predicted concentrations as a function of downstream distance. The measured data include the maximum concentration of the raw data over all times, 11-second, 20-second and 59-second averaged concentrations. For the measured data at a given downstream distance the maximum value of all sensors at that distance is taken, Sensor 14 (located at 40 m downstream, 3 meter height) has been excluded since it appeared to give erroneous too high readings

Table 2. Predicted versus observed flow rates and UDM source-term data

	Test1	Test 2	Test3	Test 5	Test6	Test 11	Test 8	Test 8R	Test 9
Discharge rate									
DISC initial discharge rate (kg/s)	8.84	10.98	9.988	50.75	3.21	7.03	4.19	3.90	6.86
DISC/TVDI discharge rate (kg/s) (averaged over first 20 seconds for tests 8,8R,9)	8.84	10.98	9.988	50.75	3.21	7.03	4.01	3.73	6.25
Observed discharge rate (kg/s) (averaged over first 20 seconds for tests 8,8R,9)	–	11.41	9.972	41.17	3.50	7.12	4.07	3.80	6.05
Deviation predicted from observed	7.8%	−3.9%	0.16%	+23%	−8.2%	−1.1%	−1.5%	−1.8%	+3.4%
Final (Post Expanded) State (UDM input)									
Discharge rate (kg/s) (from experiments)	8.2	11.41	9.988	41.17	3.50	7.12	4.07	3.80	6.05
Temperature (K) (DISC output)	194.6	194.1	194.26	194.4	193.8	194.1	198.2	204.8	194.1
Solid fraction (-) (DISC output)	0.397	0.403	0.384	0.399	0.397	0.330	0	0	0.154
Velocity (m/s) (DISC output)	156.7	189.8	179.2	191.7	191.3	154.2	466.5	472.8	289.0
'Droplet' Diameter (μm) (DISC OUTPUT)	9.35	6.53	7.29	6.16	6.54	10.0	0	0	2.82

(higher than sensors at 1 meter height and sensors further upstream). Furthermore no further analysis has been carried out (e.g. via spline fitting of the measured values to obtain a better fit of the crosswind concentration profile and a better estimate of the maximum concentration) to further refine this maximum value. The Phast predictions were found not to be affected by time-averaging effects due to plume meander (transition to passive dispersion occurring downwind of 80 m).

In the near field (<20 m) the 59-seconds averaged concentration predicted by Phast is close to the measured concentrations. This is also in line with UDM validation against previous experiments, where very close agreement was obtained in the near-field, jet-momentum dominated regime. Further downstream (at 20 meter and 40 meter) it is seen that the spread in the measured concentrations becomes larger with a larger effect of averaging time. This is because of (a) larger relative inaccuracy of the sensors, and (b) the CO_2 plume centre-line more likely to be further away from the sensor (also because of plume meander). Thus for this case, as is clearly illustrated by Figure 6, the maximum value would lead to 'too' large (rather random) value of the maximum concentration (it would increase with the release duration), while on the other hand the 59-second averaged concentration may lead to too small values.

Figure 7 includes results of UDM validation for maximum concentration versus downstream distance for the time-varying test 9 (vapour release). It is again seen that good agreement with the processed averaged experimental data is obtained. For this test, sensors 17 and 14 were considered to give possible incorrect readings for similar reasons to sensor 14 in test 11.

For a given experimental dataset, it is common practice [Hanna *et al.* (1991)] to calculate the geometric mean bias MG (averaged ratio of observed to predicted concentrations; MG < 1 over-prediction and MG > 1 under-prediction) and the geometric variance MG (variation from mean; minimum value = 1). Ideally, MG and VG would both equal 1.0. Geometric mean bias (MG) values of 0.5 and 2.0 can be thought of as a factor of 2 in over-predicting and under-predicting the mean, respectively. Likewise, a geometric variance (VG) of about 1.6 indicates scatter from observed data to predicted data by a factor of 2.

The table below includes the predictions of MG and VG for the BF DF1 experiments, where the observed concentrations have been based on 11-second averaged concentrations.

It is noted that all MG values are well within the range of [0.5, 2], and all variances less than 1.6 which is normally considered to be excellent agreement with the experimental data. Furthermore by choosing a time-averaging over

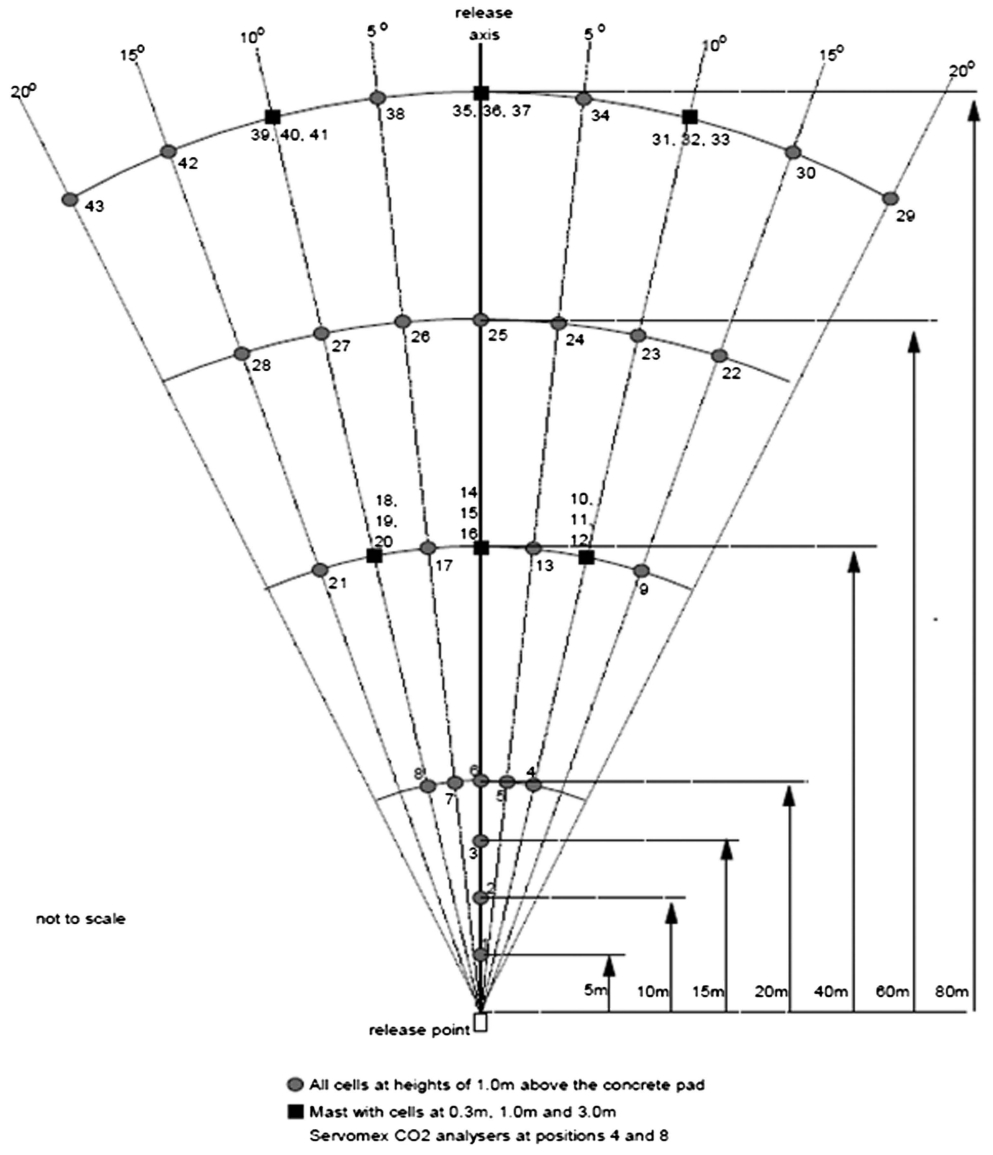

Figure 4. Field detector array for concentration and temperature measurements

11 seconds we have derived conservative estimates of the averaged observed concentrations for the cold releases (1, 2, 3, 5, 6, 11), which may (partly) explain the under-prediction of the concentrations for the experiments 2, 3, 5, 6.

For tests 1, 3, 6 there was a significant difference between the wind direction (averaged over the entire release duration) and the release direction. However the above results show that the plume centre-line did not significantly miss the sensors. Further downstream this may have been caused because we adopt 11-second averaged concentrations (maximum overall all times) rather than concentrations averaged over the entire release duration.

Furthermore it must be noted that for tests 3 and 6 a $2''$ 1.44 m extension tube was attached downstream to the $\frac{1}{2}''$ (test 3) and $\frac{1}{4}''$ (test 6) nozzle, which is not expected to affect the discharge flow rate but is likely to have affected the dispersion. This may explain the largest under-prediction of the concentrations (largest MG values) for tests 3 and test 6.

6. CONCLUSIONS AND FUTURE WORK

This paper described the validation of the Phast discharge and dispersion models against the CO2PIPETRANS JIP shared material of the BP DF1 pressurised CO_2 releases involving both steady-state cold liquid releases and time-varying supercritical hot vapour releases. The cold releases were modelled by the Phast discharge model DISC as steady-state orifice releases, while the Phast discharge model TVDI was used to model the time-varying orifice

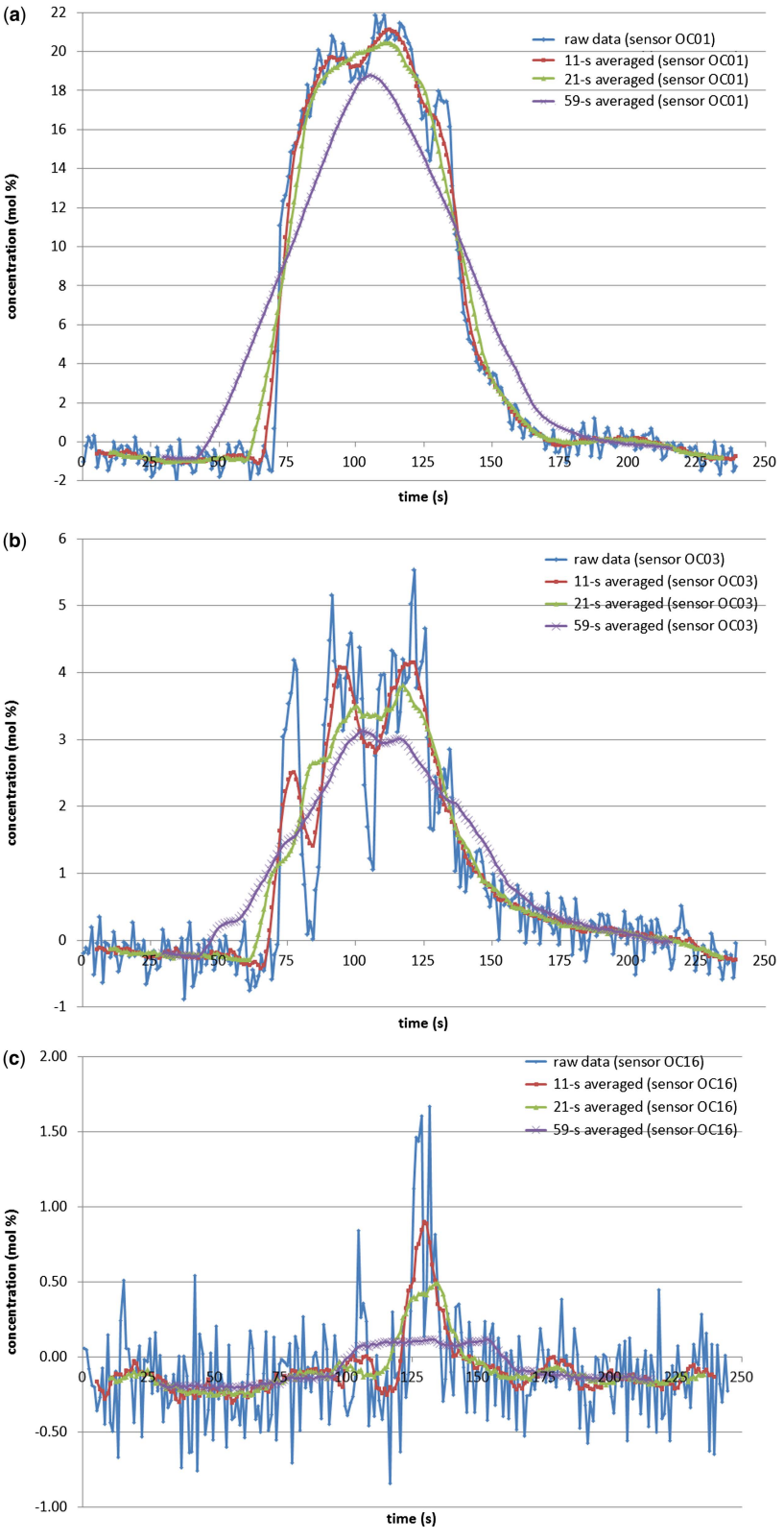

Figure 5. Test 11 – observed raw and time-averaged concentration data (a) Sensor OC01 (5m downstream) (b) Sensor OC03 (15m downstream) (c) Sensor OC16 (40m downstream)

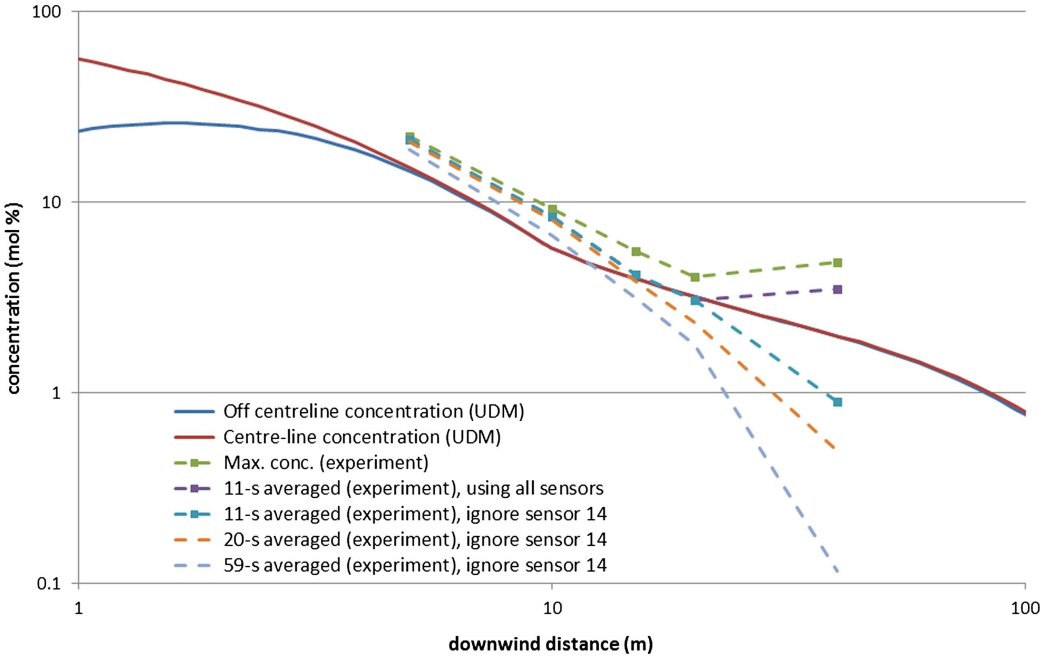

Figure 6. Test 11 – UDM validation for maximum concentration versus distance

releases. The flow rate was very accurately predicted (within a few per cent for the hot releases and within about 20% for the cold releases), which was deemed to be within the accuracy at which the experimental data were measured.

The releases were all modelled by the Phast dispersion model UDM as steady-state releases, with 20-seconds averaged flow rates applied for the time-varying releases. For all cases the solid carbon dioxide was found to sublime rapidly and no fallout was predicted, which was fully in line with the experiments. The concentrations were found to be predicted accurately (well within a factor of two).

TNo fitting of the extended Phast models has been carried out whatsoever as part of the above validation.

More recently, similar experiments to the BP DF1 experiments were carried out by GL Noble Denton funded

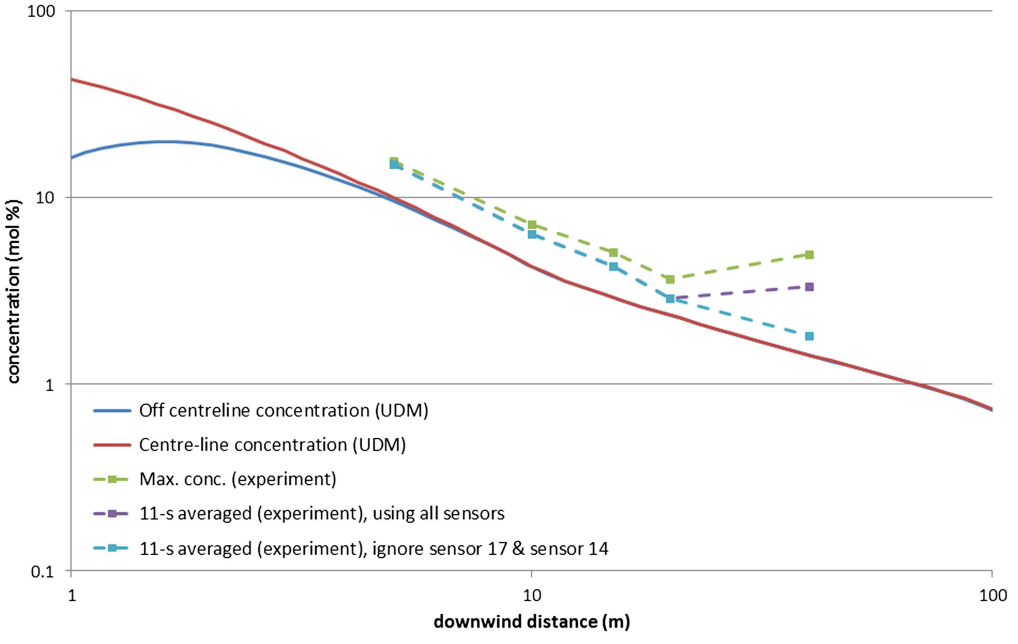

Figure 7. Test 9 – UDM validation for maximum concentration versus dist

Table 3. UDM values of mean MG and variance VG for BP DF1 CO_2 experiments

Test	Mean MG	Variance VG
1	0.89	1.18
2	1.44	1.15
3	1.60	1.30
5	1.59	1.24
6	1.63	1.31
11	0.99	1.20
8	1.25	1.07
8R	1.25	1.12
9	1.40	1.13

by Shell. The BP experimental data have been made publicly available in 2012 via the CO2PIPETRANS JIP managed by DNV (i.e. the source data for the Phast validation presented in this paper). It is hoped that the Shell data is also made public through the CO2PIPETRANS JIP. If this happens, it is expected that a separate paper will deal with the validation of Phast against the Shell experiments.

ACKNOWLEDGEMENTS

BP is acknowledged for providing funding for the initial validation of the BP DF1 experiments in 2007. The help of Hamish Holt (CO2IPETRANS JIP project manager) is acknowledged for providing input regarding the BP DF1 experiments. Finally the help of Jan Stene is acknowledged in providing feedback on the TVDI discharge calculations.

REFERENCES

Evans, J.A. and Graham, I., "DNV CO2PIPETRANS JIP — Data Release 1 — Advantica Overview", June 2012, Extract from a confidential report by Advantica for BP (2007).

Hanna, S.R., Strimaitis, D.G. and Chang, J.C. "Hazard response modelling uncertainty (A quantitative method)", Sigma Research Corp. report, Westford, MA for the API (1991).

Holt, H., "DNV CO2PIPETRANS JIP — Data Release 1 — DNV Overview Report", June 2012.

Witlox, H.W.M., "Data review and Phast analysis (discharge and atmospheric dispersion) for BP DF1 CO_2 experiments", Contract 96000056 for DNV Energy (CO2PIPETRANS Phase 2 JIP WP1), DNV Software, London (2012).

Witlox, H.W.M., Harper, M. and Holt, A., "UDM validation manual", Phast 6.7 technical documentation, DNV Software (2011).

Witlox, H.W.M., Harper, M., and Oke, A., "Modelling of discharge and atmospheric dispersion for carbon dioxide releases", Journal of Loss Prevention 22(6), 795–802 (2009).

Witlox, H.W.M., Harper, M., and Pitblado, R., "Validation of Phast dispersion model as required for USA LNG Siting Applications", LNG plant safety symposium, 12th topical conference on gas utilisation AICHE Spring Meeting, April 2012.

Witlox, H.W.M., and Holt, A., A unified model for jet, heavy and passive dispersion including droplet rainout and re-evaporation, International Conference and Workshop on Modelling the Consequences of Accidental Releases of Hazardous Materials, CCPS, San Francisco, California, September 28–October 1, pp. 315–344 (1999).

Witlox, H.W.M., and Holt, A., "Validation of the Unified Dispersion Model against Kit Fox field data", Contract 44003900 for Exxon Mobil, DNV (2001).

Witlox, H.W.M., Stene, J., Harper, M., and Nilsen, S., "Modelling of discharge and atmospheric dispersion for carbon dioxide releases including sensitivity analysis for wide range of scenarios", 10th Int. Conf. on Greenhouse Gas Control Technologies, 19–23 September 2010, Amsterdam, The Netherlands. *Made available online via Energy Procedia (Elsevier): Volume 4, 2011, pages 2253–2260.*